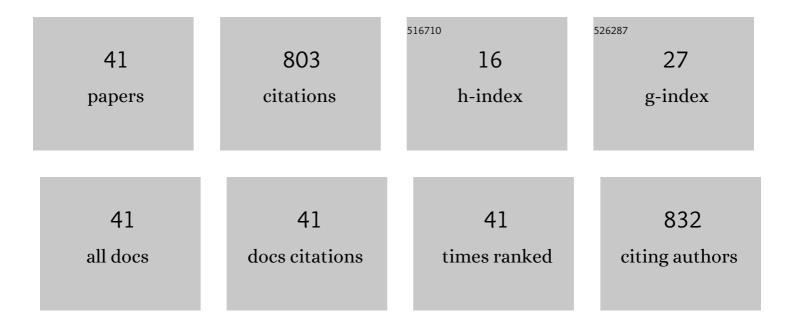
## Muhsan Ali Kalhoro

List of Publications by Year in descending order

Source: https://exaly.com/author-pdf/3627058/publications.pdf Version: 2024-02-01



#	Article	IF	CITATIONS
1	Competitive Strategy of Firms' Participation in the Global Value Chains and Labor Income Share. Complexity, 2021, 2021, 1-18.	1.6	3
2	Effects of Tropical Cyclones on Sea Surface Salinity in the Bay of Bengal Based on SMAP and Argo Data. Water (Switzerland), 2020, 12, 2975.	2.7	4
3	HY-1C Observations of the Impacts of Islands on Suspended Sediment Distribution in Zhoushan Coastal Waters, China. Remote Sensing, 2020, 12, 1766.	4.0	21
4	Variation of pCO2 concentrations induced by tropical cyclones "Wind-Pump―in the middle-latitude surface oceans: A comparative study. PLoS ONE, 2020, 15, e0226189.	2.5	8
5	A case study of Chlorophyll a response to tropical cyclone Wind Pump considering Kuroshio invasion and air-sea heat exchange. Science of the Total Environment, 2020, 741, 140290.	8.0	18
6	Interannual variability and trends in sea surface temperature, sea surface wind, and sea level anomaly in the South China Sea. International Journal of Remote Sensing, 2020, 41, 4160-4173.	2.9	14
7	The effects of ocean temperature gradients on bigeye tuna (Thunnus obesus) distribution in the equatorial eastern Pacific Ocean. Advances in Space Research, 2020, 65, 2749-2760.	2.6	4
8	Variability in phytoplankton biomass and effects of sea surface temperature based on satellite data from the Yellow Sea, China. PLoS ONE, 2019, 14, e0220058.	2.5	13
9	Satellite observations of suspended sediment near Ningbo North Dyke, China. Advances in Space Research, 2019, 64, 1415-1422.	2.6	6
10	Dissolved oxygen responses to tropical cyclones "Wind Pump" on pre-existing cyclonic and anticyclonic eddies in the Bay of Bengal. Marine Pollution Bulletin, 2019, 146, 838-847.	5.0	13
11	Chlorophyll Concentration Response to the Typhoon Wind-Pump Induced Upper Ocean Processes Considering Air–Sea Heat Exchange. Remote Sensing, 2019, 11, 1825.	4.0	36
12	Ecological response of phytoplankton to the oil spills in the oceans. Geomatics, Natural Hazards and Risk, 2019, 10, 853-872.	4.3	20
13	Study of dissolved oxygen responses to tropical cyclones in the Bay of Bengal based on Argo and satellite observations. Science of the Total Environment, 2019, 659, 912-922.	8.0	15
14	Response of Sthenoteuthis oualaniensis to marine environmental changes in the north-central South China Sea based on satellite and in situ observations. PLoS ONE, 2019, 14, e0211474.	2.5	10
15	Examining the Impact of Tropical Cyclones on Air‣ea CO <sub>2</sub> Exchanges in the Bay of Bengal Based on Satellite Data and In Situ Observations. Journal of Geophysical Research: Oceans, 2019, 124, 555-576.	2.6	22
16	Evaluation of Water Residence Time, Submarine Groundwater Discharge, and Maximum New Production Supported by Groundwater Borne Nutrients in a Coastal Upwelling Shelf System. Journal of Geophysical Research: Oceans, 2018, 123, 631-655.	2.6	31
17	Variability of aerosol optical thickness in the tropical Indian Ocean and South China Sea during spring intermonsoon season. International Journal of Remote Sensing, 2018, 39, 4531-4549.	2.9	3
18	Increased chlorophyll- <i>a</i> concentration in the South China Sea caused by occasional sea surface temperature fronts at peripheries of eddies. International Journal of Remote Sensing, 2018, 39, 4360-4375.	2.9	9

Muhsan Ali Kalhoro

#	Article	IF	CITATIONS
19	Assessment of tropical cyclone disaster loss in Guangdong Province based on combined model. Geomatics, Natural Hazards and Risk, 2018, 9, 431-441.	4.3	6
20	Stormâ€induced changes in pCO <sub>2</sub> at the sea surface over the northern <scp>S</scp> outh <scp>C</scp> hina <scp>S</scp> ea during <scp>T</scp> yphoon <scp>W</scp> utip. Journal of Geophysical Research: Oceans, 2017, 122, 4761-4778.	2.6	23
21	Detailed spatiotemporal impacts of El Niño on phytoplankton biomass in the <scp>S</scp> outh <scp>C</scp> hina <scp>S</scp> ea. Journal of Geophysical Research: Oceans, 2017, 122, 2709-2723.	2.6	8
22	Application of a generalized additive model (GAM) for estimating chlorophyll- <i>a</i> concentration from MODIS data in the Bohai and Yellow Seas, China. International Journal of Remote Sensing, 2017, 38, 639-661.	2.9	22
23	The impacts of 2008 snowstorm in China on the ecological environments in the Northern South China Sea. Geomatics, Natural Hazards and Risk, 2017, 8, 1034-1053.	4.3	6
24	Remote sensing of the impacts of construction in coastal waters on suspended particulate matter concentration – the case of the Yangtze River delta, China. International Journal of Remote Sensing, 2016, 37, 2132-2147.	2.9	15
25	World's Largest Macroalgal Blooms Altered Phytoplankton Biomass in Summer in the Yellow Sea: Satellite Observations. Remote Sensing, 2015, 7, 12297-12313.	4.0	55
26	Changes in local oceanographic and atmospheric conditions shortly after the 2004 Indian Ocean tsunami. Ocean Dynamics, 2015, 65, 905-918.	2.2	3
27	Remote sensing of spatial-temporal distribution of suspended sediment and analysis of related environmental factors in Hangzhou Bay, China. Remote Sensing Letters, 2015, 6, 597-603.	1.4	27
28	An investigation of spatial variation of suspended sediment concentration induced by a bay bridge based on Landsat TM and OLI data. Advances in Space Research, 2015, 56, 293-303.	2.6	36
29	Preliminary remote sensing observation of sea surface temperature increase during Ulva prolifera blooms. Aquatic Ecosystem Health and Management, 2014, 17, 299-304.	0.6	2
30	Northward drift of suspended sediments in the Yangtze estuary in spring. International Journal of Remote Sensing, 2014, 35, 4114-4126.	2.9	6
31	Response of dissolved oxygen and related marine ecological parameters to a tropical cyclone in the South China Sea. Advances in Space Research, 2014, 53, 1081-1091.	2.6	22
32	Enhanced seaâ€air CO <sub>2</sub> exchange influenced by a tropical depression in the <scp>S</scp> outh <scp>C</scp> hina <scp>S</scp> ea. Journal of Geophysical Research: Oceans, 2014, 119, 6792-6804.	2.6	17
33	Remote-sensing observations relevant to ocean acidification. International Journal of Remote Sensing, 2012, 33, 7542-7558.	2.9	15
34	Satellite monitoring of phytoplankton in the East Mediterranean Sea after the 2006 Lebanon oil spill. International Journal of Remote Sensing, 2012, 33, 7482-7490.	2.9	14
35	Eddy-feature phytoplankton bloom induced by a tropical cyclone in the South China Sea. International Journal of Remote Sensing, 2012, 33, 7444-7457.	2.9	75
36	Phytoplankton bloom over the Northwest Shelf of Australia after the <i>Montara</i> oil spill in 2009. Geomatics, Natural Hazards and Risk, 2011, 2, 329-347.	4.3	12

#	Article	IF	CITATIONS
37	Analysis of the spatio-temporal distribution of chlorophyll-a in the eastern Indian Ocean near the time of the 2004 South Asian tsunami. International Journal of Remote Sensing, 2010, 31, 4579-4593.	2.9	4
38	Remote sensing of day/night sea surface temperature difference related to phytoplankton blooms. International Journal of Remote Sensing, 2010, 31, 4569-4578.	2.9	12
39	Onshore–offshore variations of copepod community in northern South China Sea. Hydrobiologia, 2009, 636, 257-269.	2.0	27
40	Variations of chlorophyll- <i>a</i> in the northeastern Indian Ocean after the 2004 South Asian tsunami. International Journal of Remote Sensing, 2009, 30, 4553-4565.	2.9	23
41	Occurrences of harmful algal blooms (HABs) associated with ocean environments in the South China Sea. Hydrobiologia, 2008, 596, 79-93.	2.0	123